

Electrical signals for chondrocytes in cartilage

W.M. Lai, D.D. Sun, G.A. Ateshian, X.E. Guo and V.C. Mow

Departments of Mechanical Engineering, Orthopaedic Surgery and Biomedical Engineering, Columbia University, New York, NY 10027, USA

Tel.: +1 212 854 4236; Fax: +1 212 854 4404; E-mail: WML1@Columbia.edu

Abstract. An important step toward understanding signal transduction mechanisms modulating cellular activities is the accurate predictions of the mechanical and electro-chemical environment of the cells in well-defined experimental configurations. Although electro-kinetic phenomena in cartilage are well known, few studies have focused on the electric field *inside* the tissue. In this paper, we present some of our recent calculations of the electric field *inside* a layer of cartilage (with and without cells) in an open circuit one-dimensional (1D) stress relaxation experiment. The electric field inside the tissue derives from the streaming effects (streaming potential) and the diffusion effect (diffusion potential). Our results show that, for realistic cartilage material parameters, due to deformation-induced inhomogeneity of the fixed charge density, the two potentials compete against each other. For softer tissue, the diffusion potential may dominate over the streaming potential and vice versa for stiffer tissue. These results demonstrate that for proper interpretation of the mechano-electrochemical signal transduction mechanisms, one must not ignore the diffusion potential.

1. Introduction

The biologic activities of the chondrocyte population are regulated by genetic, and other biologic and biochemical factors, as well as environmental factors. It has often been noted that physical environmental factors, such as stress, flow, electric field, etc. are as strong as biologic factors in regulating cellular activities [10,21]. In recent years, there has been much research on the effects of mechanical and/or hydrostatic/osmotic pressure loading on cartilage explant metabolism (see [21] and [11] and the references therein). Such studies have been specifically aimed at elucidating possible “mechano-signal” transduction mechanism(s) that might govern the chondrocytes’ biosynthetic activities in maintaining and organizing the extracellular matrix (ECM) comprising the tissue (see the reviews by Comper [3], and Mow and Ratcliffe [22]). Although the electrical events in cartilage have been observed by many researchers for more than three decades [1,2,5–8,13,17–20], few studies however have focused on the details of the electrical potential *within* the ECM where the chondrocytes reside. The development of more elaborate constitutive models of cartilage in recent years has enabled us to calculate the various mechanical and electrical signals that the chondrocytes might see *in situ* [16]. In this paper, we present some of the results that we have obtained for the electric field in and around a cell inside a tissue under a 1D stress relaxation experimental configuration. The contribution of diffusion potential to the total potential field, ignored by most cartilage researcher, is also assessed.

2. Streaming potential and diffusion potential in the absence of electric current

Using the triphasic theory [15], one can derive the following equation for the electric current density in cartilage (see also [9] and [12])

$$I_e = -g_o \nabla P - \frac{RT}{F_c} \left[\sum_{\alpha=+,-} g_\alpha \nabla (\ln (\gamma_\alpha c^\alpha)) \right] - \chi_o \nabla \psi, \quad (1)$$

where P is the pressure (hydraulic and osmotic), c^+ and c^- are cation and anion concentrations (per unit tissue water volume), γ_α are activity coefficients, F_c is Faraday constant, ψ is electric potential, R is universal gas constant, T is absolute temperature, g_o , g_α and χ_o are material parameters which are functions of the ion concentrations and the frictional coefficients. Equation (1) states that the electric current density at any point is the vector sum of three kinds of currents: the convection current (the first term on the right-hand side of Eq. (1)), the diffusion current (the second term) and the conduction current (the last term). The driving force for the convection current is the mechano-chemical force ∇P , generated by the gradient of the pressures. The driving force for the diffusion current is the electro-chemical force $\nabla(\gamma_\alpha c^\alpha)$, generated by the gradient of the concentration c^α for the ionic species; and the driving force for the conduction current is the electric force $\nabla \psi$, generated by the gradient of the electric potential ψ . The fluid flow, driven by the pressure gradient, convects the cations and anions (of unequal concentration), resulting in a *convection current*. The diffusion of cations and anions at different speeds or at different directions, driven by the gradient of concentrations, results in a *diffusion current*, and the movements of ions under a non-zero gradient of electric potential ψ give rise to a *conduction current*. When external circuits are not provided for the tissue to sustain a net flow of ions and electrons, the tissue is in a state of zero current. This condition is the most commonly used experimental configuration in the study of charged biological tissues for the determination of their electrical behaviors. For such cases, at every point in the tissue, the sum of the three currents must vanish. In this currentless experimental condition, there is no externally applied electric potential, the potential is entirely *induced* by the convection current and the diffusion current. This induced potential generates a conduction current to oppose the convection current and the diffusion current so as to achieve the zero current condition. The potential induced by convection in the presence of a pressure gradient is the *streaming potential*. The potential induced by the diffusion in the presence concentration gradient is the *diffusion potential*.

3. Confined compression stress relaxation experiment in and around a cell

The length scale for cells differs from that for the tissue by more than two orders of magnitude (~ 1 mm for the tissue and $\sim 10 \mu\text{m}$ for the cell), therefore, it is necessary to use a two-scale finite-element model to analyze the events surrounding a cell. In the following, we first present our parametric study of the macro-scale problem so as to gain understanding on the relative importance of streaming and diffusion potential in this problem. The parameter that has an important effect on the diffusion potential is the intrinsic aggregate modulus H_a of the ECM.

3.1. Macroscale problem (ECM in the absence of cells)

A schematic diagram for a 1D ramped displacement stress relaxation experiment is shown in Fig. 1. The layer of tissue is confined within a rigid-cylindrical container. The side-wall and bottom are insulated

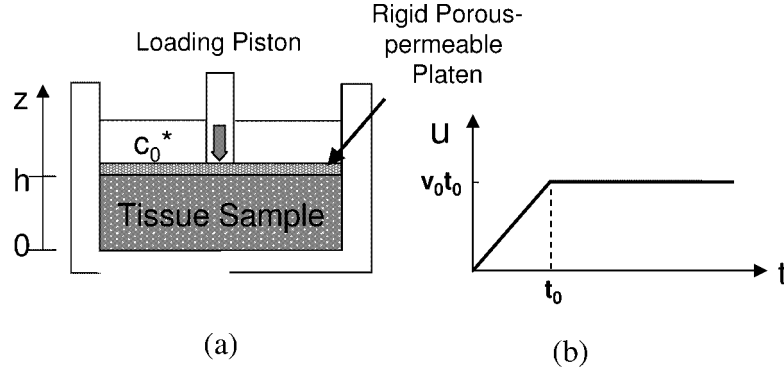


Fig. 1. (a) Schematic of an open-circuit, 1D ramped-displacement, stress-relaxation experiment. The bathing NaCl solution concentration c^* is kept fixed during the experiment, and the motion of the loading piston is prescribed in (b). The surface-to-surface compressive strain is 10%, $t_0 = 200$ s and $h = 1$ mm.

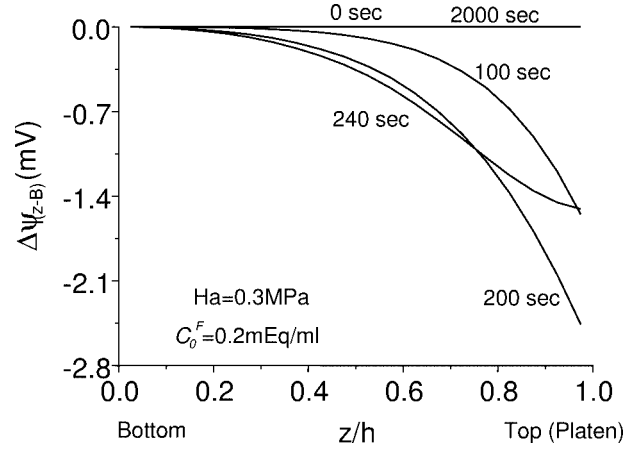


Fig. 2. Electric potential distribution *inside* the tissue at various times for $H_a = 0.3$ MPa. The potential increases in the direction toward the bottom indicating that it is dominated by the diffusion potential. Initial FCD $c_0^F = 0.2$ mEq/ml; diffusivities of Na^+ and Cl^- are 0.5×10^{-9} and 0.8×10^{-9} m^2/s , respectively, porosity $\phi_0^w = 0.8$, friction coefficient between water and solid matrix $K = 7 \times 10^{14}$ $\text{N s}/\text{m}^4$.

against flow of water and ions. Compressing the tissue from its top is a rigid porous-permeable loading platen. The ramped-displacement imposed on this loading platen is given in Fig. 1(b). The tissue is initially equilibrated in a NaCl solution of concentration $c^* = 0.15$ M NaCl. Prior to the application of the ramped displacement $U(t)$, the tissue is in equilibrium where the anions distribution is given by the Donnan equilibrium distribution law $c^+(z, 0)c^-(z, 0) = \gamma_{\pm}^2 c^{*2}$ [19,22]. With v^α ($\alpha = s, +$ and $-$) denoting the velocity of solid, cation and anion, respectively, the currentless condition (open circuit) is expressed as $c^+(v^+ - v^s) = c^-(v^- - v^s)$. The solution of this problem is obtained using the finite element formulation of Sun et al. [23].

Figure 2 shows the electric potential distribution $\Delta\psi_{z-B} [= \psi(z, t) - \psi(0, t)]$ at various times, for a tissue with aggregate modulus $H_a = 0.3$ MPa. It is seen here that $\Delta\psi_{z-B}$ is negative for all times, that is $\psi(0, t) \geq \psi(z, t)$ so that the electric potential increases from porous platen toward the bottom of the specimen, indicating that the diffusion potential dominates over the streaming potential. This large diffusion potential effect is due to the compaction of the charged solid matrix (see Fig. 3), caused by the

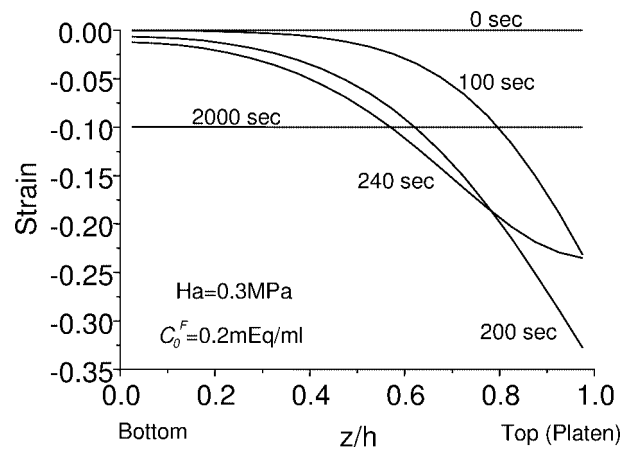


Fig. 3. Strain distribution *inside* the tissue at various times. The strain is caused by frictional drag force of permeation between water and solid matrix. The strain increases monotonically in the upward (flow) direction, so does the FCD (not shown).

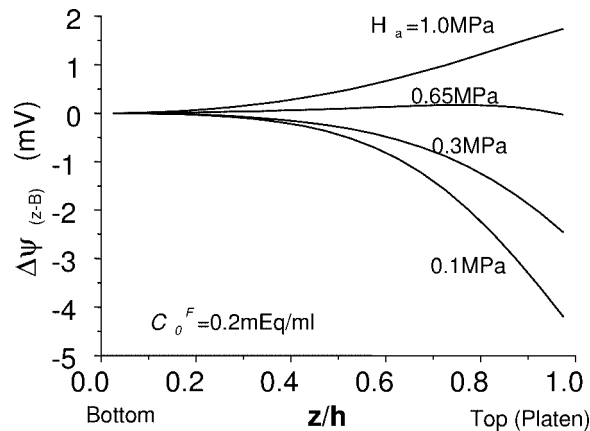


Fig. 4. Electric potential distribution *inside* the tissue at time $t = 200$ s (i.e., at the end of the compression-ramp phase) for four values of aggregate modulus. For more rigid tissue ($H_a > 0.65$ MPa), the streaming potential effect dominates whereas for softer tissues ($H_a < 0.65$ MPa), the diffusion potential effect dominates.

drag forces, exerted by the fluid on the solid matrix, during the ramped-phase of the experiment [14]. For tissues with larger compressive stiffness, the opposite may be true, i.e., the streaming potential dominates with more positive potential near the loading platen. The electric potential for four values of aggregate modulus H_a are shown in Fig. 4. The results show that the electric fields inside the tissue reverse its polarity at approximately $H_a = 0.65$ MPa.

3.2. Microscale problem – electric field in and around a cell

Once the macro-scale model is solved, its solid displacement, water and ion chemical/electrochemical potentials are then used to define the boundary conditions at the interface of the micro-scale cell–matrix model. In the following we discuss the results of our calculation using this two-scale approach. The chondrocyte is assumed to be spherical with a radius = $5 \mu\text{m}$. Due to the sparse population of chondrocytes in articular cartilage (10% in volume in mature tissue [24]), only one chondrocyte is assumed

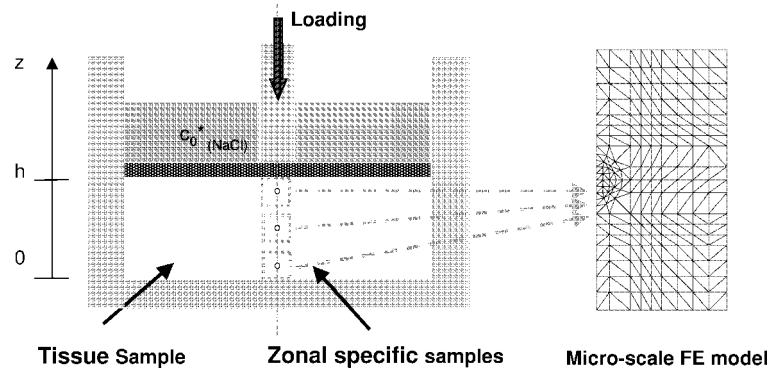


Fig. 5. The schematic representations of the two-scale triphasic finite element model for tissue and cell. The right figure is the micro-scale model.

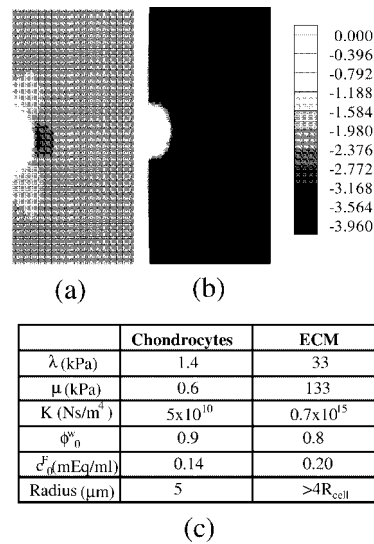


Fig. 6. The contour plots of the electric field in and around a cell at the ramp peak: (a) Cell near the tissue surface. (b) Cell at the middle zone depth. The electrical potential shown is relative to the center of the cell. (c) Properties of ECM and chondrocyte are listed in the table, where λ and μ are Lamé constants for the solid phase.

to be embedded inside the micro-scale tissue domain (Fig. 5). That is, we assume that the interactions between and among chondrocytes are negligible. The cell is also modeled as a triphasic medium but with different material parameters from those of the ECM, as represented in the literature [11]. Further, it is assumed that the cell adheres to the ECM. The cell–matrix domain is chosen to be 5 times of the cell radius. The external bathing solution was chosen to be 0.15 M NaCl solution. The calculated results show that the electric field depends on the location of the cell in the tissue as well as time. For example, at the peak of the ramped displacement, the electrical potential difference between the territorial matrix and the center of the cell is -2.2 mV for a cell near the surface versus -4.2 mV for a cell at 1/2 depth from the surface. It should be noted that the cell near the surface was compressed more than the cell at mid-depth so that the difference in FCD between the cell and ECM is less for the cell near the surface. For a complete picture of the electric field surrounding a cell, we show in Fig. 6 a contour plot of the electric field (relative to the center of the cell) in and around a cell in the surface zone.

4. Conclusions

The triphasic theory is used to provide a complete description of the electric field in and around a cell inside a layer of tissue in 1D confined compression stress relaxation experiment. In the theory, both the streaming potential and the diffusion potential effects are included. We found that for cartilage ECM, these two potentials may be of the same order of magnitudes, and compete *against* each other under realistic loading conditions. Thus, for proper interpretation of the signal transduction data, one must not ignore the diffusion potential in the theory.

Acknowledgement

This work was supported in part by NIH Grant No.: AR41913, and No.: AR42850.

References

- [1] C.A.L. Bassett and R.J. Pawluk, Electrical behavior of cartilage during loading, *Science* **178** (1972), 982–983.
- [2] A.C. Chen, T.T. Nguyen and R.L. Sah, Streaming potentials during the confined compression creep test of normal and proteoglycan-depleted cartilage, *Ann. Biomed. Eng.* **25** (1997), 269–277.
- [3] W.D. Comper, *Extracellular Matrix*, Vol. 2, Harwood Academic Publishers, Australia, 1996, pp. 1–386.
- [4] F.G. Donnan, The theory of membrane equilibria, *Chem. Rev.* **1** (1924), 73–90.
- [5] E.H. Frank, A.J. Grodzinsky, T.J. Koob and D.R. Eyre, Streaming potentials: A sensitive index of enzymatic degradation in articular cartilage, *J. Orthop. Res.* **5** (1987), 497–508.
- [6] E.H. Frank and A.J. Grodzinsky, Cartilage electromechanics. I. Electrokinetic transduction and the effects of electrolyte pH and ionic strength, *J. Biomechanics* **20** (1987), 615–627.
- [7] A.J. Grodzinsky, H. Lipshitz and M.J. Glimcher, Electromechanical properties of articular cartilage during compression and stress relaxation, *Nature* **275** (1978), 448–450.
- [8] W.Y. Gu, W.M. Lai and V.C. Mow, Transport of fluid and ions through a porous-permeable charged-hydrated tissue, and streaming potential data on normal bovine articular cartilage, *J. Biomechanics* **26** (1993), 709–723.
- [9] W.Y. Gu, W.M. Lai and V.C. Mow, A mixture theory for charged hydrated soft tissues containing multi-electrolytes: passive transport and swelling behaviors, *J. Biomech. Engng.* **120** (1998), 169–180.
- [10] F.A. Guilak, R.L. Sah and L.A. Setton, Physical regulation of cartilage metabolism, *Basic Orthopaedic Biomechanics*, V.C. Mow and W.C. Hayes, eds, Lippincott-Raven Pubs, Philadelphia, 1997, pp. 179–207.
- [11] F. Guilak and V. Mow, The mechanical environment of chondrocyte: a biphasic finite element model of cell–matrix interactions in articular cartilage, *J. Biomechanics* **33** (2000), 1663–1673.
- [12] J.M. Huyghe, J.D. Janssen, Quadriphasic mechanics of swelling incompressible porous media, *Int. J. Engng. Sci.* **35** (1997), 793–802.
- [13] Y.J. Kim, L.J. Bonassar and A.J. Grodzinsky, The role of cartilage streaming potential, fluid flow and pressure in the stimulation of chondrocyte biosynthesis during dynamic compression, *J. Biomechanics* **28** (1995), 1055–1066.
- [14] W.M. Lai and V.C. Mow, Drag-induced compression of articular cartilage during permeation experiment, *Biorheology* **17** (1980), 111–123.
- [15] W.M. Lai, J.S. Hou and V.C. Mow, A triphasic theory for swelling and deformation behavior of articular cartilage, *J. Biomech. Engng.* **113** (1991), 245–258.
- [16] W.M. Lai, V.C. Mow, D.N. Sun and G.A. Ateshian, On the electric potentials inside a charged soft hydrated biological tissue: Streaming potential vs. diffusion potential, *J. Biomech. Engng.* **122** (2000), 336–346.
- [17] R.C. Lee, E.H. Frank, A.J. Grodzinsky and D.K. Roylance, Oscillatory compressional behavior of articular cartilage and its associated electromechanical properties, *J. Biomech. Engng.* **103** (1981), 280–292.
- [18] P.A. Lotke, J. Black and S.J. Richardson, Electromechanical properties in human articular cartilage, *J. Bone Joint Surgery* **56A** (1974), 1040–1046.
- [19] A. Maroudas, Physicochemical properties of cartilage in the light of ion exchange theory, *Biophys. J.* **8** (1968), 575–595.
- [20] A. Maroudas, H. Muir and J. Wingham, The correlation of fixed negative charge with glycosaminoglycan content of human articular cartilage, *Biochim. Biophys. Acta* **177** (1969), 492–500.
- [21] V.C. Mow, C.B. Wang and C.T. Hung, The extracellular matrix, interstitial fluid and ions as a mechanical signal transducer in articular cartilage, *Osteoarthritis Cart.* **7** (1999), 41–58.

- [22] V.C. Mow and A. Ratcliffe, Structure and function of articular cartilage and meniscus, in: *Basic Orthopaedic Biomechanics*, V.C. Mow and W.C. Hayes, eds, Lippincott-Raven Pubs, Philadelphia, 1997, pp. 113–177.
- [23] D.N. Sun, W.Y. Gu, X.E. Guo, W.M. Lai and V.C. Mow, A mixed finite element formulation of triphasic mechano-electrochemical theory for charged, hydrated biological soft tissues, *Int. J. Num. Meth. Eng.* **45** (1999), 1375–1402.
- [24] R.A. Stockwell, *Biology of Cartilage Cells*, Cambridge University Press, Cambridge, 1979.